Exposing the hidden topology of multiple Hartree–Fock states

Hugh G. A. Burton* and Alex J. W. Thom
Department of Chemistry, University of Cambridge, Lensfield Road, Cambridge, CB2 1EW, U.K.
(Dated: September 16, 2018)

Self-consistency in the Hartree–Fock equations results in multiple non-orthogonal solutions that need not share the symmetries of the true Hamiltonian. Our current understanding into the nature of these multiple solutions is relatively limited. We propose a non-Hermitian analytic continuation of real Hartree–Fock as a framework for understanding the topology of multiple Hartree–Fock solutions. We then apply this framework in the periodic Hubbard chain to reveal complex connections between symmetry-broken Hartree–Fock states as part of a continuous manifold of solutions. Finally, we identify and explain the appearance of self-orthogonal solutions in Hartree–Fock.

Hartree–Fock theory performs a pivotal role in quantum chemistry, providing a mean-field description of electronic structure in terms of a single Slater determinant upon which electron correlation can be computed.[1] As a non-linear self-consistent field (SCF) approach, the Hartree–Fock equations have the potential to produce a multitude of different solutions. Despite the development of effective techniques for locating multiple SCF solutions — for example SCF Metadynamics,[2] homotopy approaches[3] and the Maximum Overlap Method[4] — our understanding into the general nature of multiple Hartree–Fock states remains surprisingly limited.

Initially, the importance of multiple SCF solutions was emphasised by the stability analysis pioneered by Thouless[5], Čížek and Paldus[6, 7], and Seeger and Pople[8]. Through stability analysis, along with the work of Fukutome,[9] Hartree–Fock solutions were classified in terms of the self-consistent symmetries they preserve, as reviewed by Stuber and Paldus.[10] The self-consistency of the Hartree–Fock equations, however, can also lead to symmetry-broken solutions, resulting in Löwdin's "symmetry dilemma"[11]; should one seek the lowest energy solution whilst sacrificing the good quantum numbers offered by symmetry-pure states? Moreover, the onset of symmetry breaking is accompanied by the coalescence, or emergence, of solutions at instability thresholds,[12, 13] and appears intimately linked with the degree of strong correlation present. The most notorious example remains the Coulson–Fischer point in the dissociation of H_2, where the ground state restricted Hartree–Fock (RHF) solution splits spontaneously into two unrestricted Hartree–Fock (UHF) solutions breaking both point-group and $\hat{S}^2$ symmetry.[14]

Elsewhere in quantum physics, non-Hermitian Hamiltonians have recently been developed as a framework for understanding the nature of multiple eigensolutions. Non-Hermitian approaches, including non-Hermitian Hartree–Fock[15], have traditionally been limited to the description of time-dependent phenomena requiring complex eigenvalues, for example ionisation, dissociation and metastable resonance states.[16] However, Bender and Boettcher[17] have introduced non-Hermitian Hamiltonians as an approach for understanding multiple eigenstates in quantum systems through the framework of complex analytic continuation. Using this technique, a real-symmetric Hamiltonian is analytically continued into the complex plane, becoming non-Hermitian in the process and exposing the fundamental topology of the Hamiltonian's eigenstates. Quantised eigenvalues, for example, emerge directly from the discrete nature of sheets contained within a Riemann surface.[18] Moreover, when eigenstates of a linear non-Hermitian Hamiltonian coincide at a branch point, non-intuitive self-orthogonal eigenstates that satisfy $\langle\psi^*|\psi\rangle = 0$ can arise.[16] Further exploiting the framework of branch points and branch cuts also reveals complex connections between eigenstates, creating an elegant arena in which a deeper understanding of quantum theory can be developed.[19, 20]

To our knowledge, the topology of multiple Hartree–Fock solutions remains unexplored in the framework of analytic continuation. Recently, with the ambition of utilising multiple Hartree–Fock states as a basis for non-orthogonal configuration interaction,[21] the holomorphic Hartree–Fock approach has been developed as a method for analytically continuing real Hartree–Fock solutions beyond the instability thresholds at which they vanish.[22, 23] In holomorphic Hartree–Fock theory, the complex conjugation of orbital coefficients is removed from the conventional Hartree–Fock equations, resulting in a non-Hermitian Hamiltonian with a complex analytic energy function. Holomorphic Hartree–Fock solutions are then found to exist across all molecular geometries, obtaining complex valued orbital coefficients even when their real counterparts coalesce and disappear.[22–24]

Previously, the holomorphic Hartree–Fock approach has proved useful for exploring the maximum number of solutions of closed-shell two-electron systems.[24] In this work, we demonstrate how the non-Hermiticity of holomorphic Hartree–Fock theory provides a wider, general framework for understanding the topology of multiple Hartree–Fock solutions. We begin by reviewing the mathematical details of holomorphic Hartree–Fock theory. We then explore the holomorphic Hartree–Fock solutions of the one-dimensional Hubbard chain, drawing parallels with non-Hermitian physics and exposing previ-

ously unseen connections between real symmetry-broken states through the complex plane.

In what follows, we utilise the holomorphic RHF (h-RHF) approach as an example, although the method can be extended to all real formalisms of Hartree–Fock. Consider a closed-shell system comprising $2N$ electrons and a set of N doubly-occupied orbitals $\{|\phi_i\rangle\}$. Employing the tensor notation of Head-Gordon *et al.*[25] each orbital can be constructed from a finite linear combination of n orthonormalised real single-particle basis functions $\{|\chi_\mu\rangle\}$ as $|\phi_i\rangle = \sum_\mu^n |\chi_\mu\rangle\, C_{\cdot i}^{\mu\cdot}$. In conventional RHF theory, the energy E for this system is given by

$$E = h_{\text{nuc}} + 2\sum_{i}^{N}\sum_{\mu\nu}^{n} (C^*)_{i\cdot}^{\cdot\mu}\, h_{\mu\nu} C_{\cdot i}^{\nu\cdot} + \sum_{ij}^{N}\sum_{\mu\nu\sigma\tau}^{n} (C^*)_{i\cdot}^{\cdot\mu}\,(C^*)_{j\cdot}^{\cdot\nu}\Big[2\langle\mu\nu|\sigma\tau\rangle - \langle\mu\nu|\tau\sigma\rangle\Big] C_{\cdot i}^{\sigma\cdot} C_{\cdot j}^{\tau\cdot}, \tag{1}$$

where h_{nuc} is the nuclear repulsion, and $h_{\mu\nu}$ and $\langle\mu\nu|\sigma\tau\rangle$ are the one- and two-electron integrals respectively, expressed in the basis $\{|\chi_\mu\rangle\}$. RHF solutions exist as stationary points of Equation 1 subject to the orthogonality constraint

$$\sum_{\mu}^{n} (C^*)_{i\cdot}^{\cdot\mu}\, C_{\cdot j}^{\mu\cdot} = \delta_{ij}. \tag{2}$$

When the orbital coefficients are considered over the full complex domain, Equation 1 and Equation 2 become functions of several complex variables $\{C_{\cdot i}^{\mu\cdot}\}$ and their complex conjugates $\{(C^*)_{\cdot i}^{\mu\cdot}\}$. However, this dependence on $\{(C^*)_{\cdot i}^{\mu\cdot}\}$ violates the Cauchy–Riemann conditions,[26] resulting in functions that are not complex analytic and rendering conventional complex Hartree–Fock theory unsuitable as a framework for exploring the topology of real Hartree–Fock solutions.

In contrast, the h-RHF energy $\widetilde{E}$ is defined[22] as an analytic function of the complex orbital coefficients by removing the complex conjugation in Equation 1 to yield

$$\widetilde{E} = h_{\text{nuc}} + 2\sum_{i}^{N}\sum_{\mu\nu}^{n} C_{i\cdot}^{\cdot\mu} h_{\mu\nu} C_{\cdot i}^{\nu\cdot} + \sum_{ij}^{N}\sum_{\mu\nu\sigma\tau}^{n} C_{i\cdot}^{\cdot\mu} C_{j\cdot}^{\cdot\nu}\Big[2\langle\mu\nu|\sigma\tau\rangle - \langle\mu\nu|\tau\sigma\rangle\Big] C_{\cdot i}^{\sigma\cdot} C_{\cdot j}^{\tau\cdot}. \tag{3}$$

From this definition, both the holomorphic density matrix $\widetilde{P}^{\mu\nu} = \sum_i^N C_{\cdot i}^{\mu\cdot} C_{i\cdot}^{\cdot\nu}$ and its corresponding holomorphic Fock matrix $\widetilde{F}$ form non-Hermitian, complex-symmetric matrices.[23] Consequently, the eigenvectors of $\widetilde{P}$ and $\widetilde{F}$ (representing the holomorphic single-particle orbitals) form a complex orthogonal set[27] and the orthogonality constraint condition becomes

$$\sum_{\mu}^{n} C_{i\cdot}^{\cdot\mu} C_{\cdot j}^{\mu\cdot} = \delta_{ij}. \tag{4}$$

The stationary points of the h-RHF equations can be identified using a modified SCF approach,[23] and it has previously been shown that when real Hartree–Fock solutions disappear, their holomorphic counterparts continue to exist with complex orbital coefficients.[22–24]

When the orbital coefficients are real, the conventional and holomorphic energy expressions become equivalent, and the two formalisms share the same set of solutions. However, when the orbital coefficients are allowed to become complex, the two approaches diverge, with the holomorphic Hartree–Fock method forming the rigorous analytic continuation of the real Hartree–Fock equations. Consequently, in contrast to conventional complex Hartree–Fock, the holomorphic formalism provides the perfect non-Hermitian framework for understanding the topology of real Hartree–Fock states.

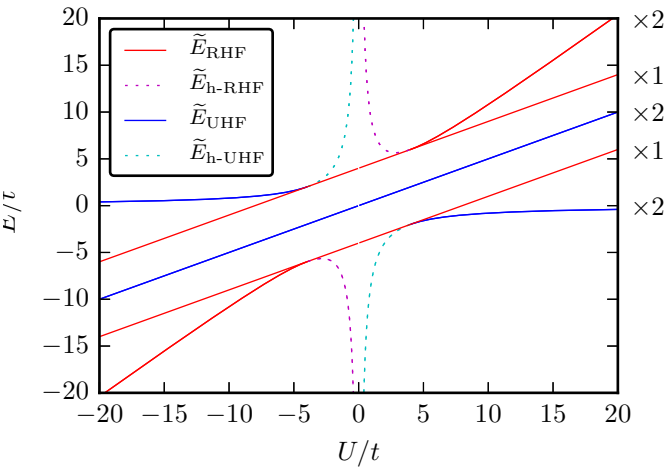

FIG. 1: Holomorphic energy of the multiple holomorphic solutions to the periodic two-electron, two-site Hubbard chain with their degeneracies. At $U/t = 20$, the state symmetries in ascending energy are: symmetry-broken; σ_{g}^2; $\sigma_{\text{g}}\sigma_{\text{u}}$; σ_{u}^2; and symmetry-broken.

The one-dimensional, periodic Hubbard model[28] provides an ideal system for exploring the topology of Hartree–Fock solutions. We consider the wavefunction expanded in a basis set of orthogonal orbitals $\{|\chi_\mu\rangle\}$, each localised on a lattice site of an n-site chain. Expressed within this basis, the one-electron integrals are parameterised by the hopping term t as $h_{\mu\nu} = -t\,(\delta_{\mu,\nu+1} + \delta_{\mu,\nu-1})$, where periodic boundary conditions must be respected, whilst the only non-zero two-electron integrals are given by the on-site Coulombic repulsion $\langle\mu\nu|\sigma\tau\rangle = U\delta_{\mu\nu}\delta_{\nu\sigma}\delta_{\sigma\tau}$. Taking t as the unit of energy then leaves the ratio U/t as the only system parameter, representing the electron correlation strength. Allowing

U/t to take both negative and positive values leads to the attractive and repulsive Hubbard models respectively.

For ease of conceptual understanding and visualisation, we limit our in-depth analysis to two-electron systems at the h-RHF level of theory. The h-UHF solutions are included for completeness only. Since we operate in the space of occupied-virtual orbital rotation angles, our discussion generalises easily to unrestricted or many-electron systems.

Take first a two-site, two-electron lattice, represented at the h-RHF level of theory by the single doubly-occupied orbital $|\phi_1\rangle$. Satisfaction of the complex-orthogonality constraint, Equation 4, can be ensured by parameterising $|\phi_1\rangle$ in terms of the complex angle θ_1 as

$$|\phi_1\rangle = |\chi_1\rangle \cos\theta_1 + |\chi_2\rangle \sin\theta_1. \tag{5}$$

Since the holomorphic energy and density are both invariant to the overall sign symmetry $(\cos\theta_1, \sin\theta_1) = (-\cos\theta_1, -\sin\theta_1)$, only the domain $\theta_1 \in X$, where $X = \{x \in \mathbb{C} : -\frac{\pi}{2} \leq \mathrm{Re}[x] < \frac{\pi}{2}\}$, needs to be considered. The holomorphic energy $\widetilde{E}$ can then be expressed using the trigonometric function

$$\widetilde{E} = -8t \cos\theta_1 \sin\theta_1 + U\left(\cos^4\theta_1 + \sin^4\theta_1\right). \tag{6}$$

Optimising Equation 6 produces h-RHF states as the roots of

$$\frac{\mathrm{d}\widetilde{E}}{\mathrm{d}\theta_1} = -2\cos 2\theta_1 \left(U \sin 2\theta_1 + 4t\right), \tag{7}$$

which, upon factorisation, yields solutions at

$$\theta_1 = \frac{1}{2}\arccos 0, \tag{8}$$

$$\theta_1 = \frac{1}{2}\arcsin\left(-\frac{4t}{U}\right). \tag{9}$$

To satisfy $\theta_1 \in X$ the range of arccos and arcsin must be extended over $Y = \{y \in \mathbb{C} : -\pi \leq \mathrm{Re}[y] < \pi\}$, and both Equation 8 and Equation 9 must be considered as multi-valued functions. Consequently, a total of four h-RHF solutions can be identified, shown in Figure 1 alongside a further four h-UHF states. For the case of Equation 8 these solutions correspond trivially to $\theta_1 = -\pi/4$ and $\theta_1 = \pi/4$, representing the parity-symmetric σ_u^2 and σ_g^2 states respectively[29]. The solutions to Equation 9, however, are dictated by the strength of the correlation. In the strong correlation limit, $U/t \to \pm\infty$, the critical values are given by $\theta_1 \to 0$ and $\theta_1 \to -\pi/2$, representing degenerate parity-broken states with the electron pair localised on site-1 and site-2 respectively. These states, mutually related by symmetry, increasingly delocalise as the correlation strength is lowered until eventually coalescing at the Coulson–Fischer points $(U/t)_{\mathrm{CFP}} = \pm 4$. For $|U/t| < 4$, the critical values of θ_1 become complex, and the holomorphic solutions continue as a parity-broken, complex-conjugate pair.

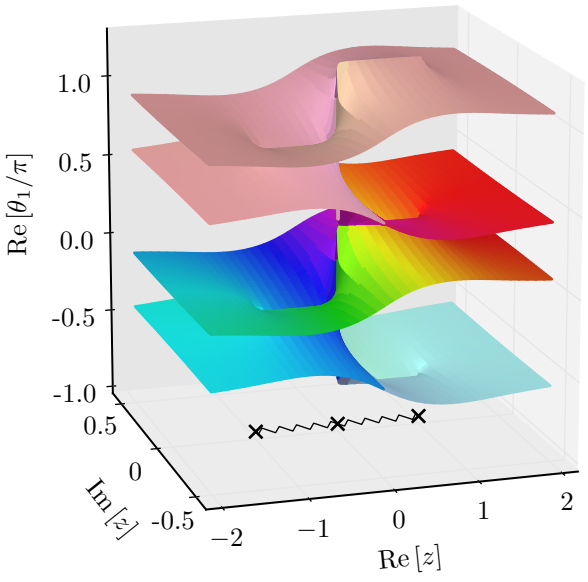

FIG. 2: Riemann surface representing the parity-broken solutions of the two-site Hubbard chain as solutions to Equation 10. Domain colouring indicates $\arg\theta_1$, and the first periodic repeat of each state is plotted to emphasise the overall structure (faded regions). The branch cuts from $z = -1$ to $z = 0$ and $z = 0$ to $z = 1$ are shown beneath the Riemann surface.

Such a description, however, provides only a tantalising glimpse into the full topology of the multiple parity-broken Hartree–Fock states. To reveal the complete picture, U/t itself must be analytically continued into the complex plane and the solutions to Equation 9 expressed using the complex logarithm

$$\theta_1 = -\frac{\mathrm{i}}{2}\ln\left(\frac{\mathrm{i} + \sqrt{z^2 - 1}}{z}\right), \tag{10}$$

where $z = -U/(4t)$. From the form of Equation 10, two branch points can be identified corresponding to the Coulson–Fischer points at $z = \pm 1$, along with a logarithmic branch point at $z = 0$. As a result, the full set of parity-broken h-RHF solutions for both the repulsive and attractive Hubbard model can be represented by an infinitely-sheeted Riemann surface with branch-cuts extending from $z = -1$ to 0 and from $z = 0$ to $+1$, as shown in Figure 2. From this single Riemann surface, an underlying connection of the real parity-broken h-RHF solutions elegantly emerges through the complex plane; as the branch points at $z = \pm 1$ are circumscribed across a branch cut, the two symmetry-related states that coalesce at the Coulson–Fischer points are analytically interconverted. Moreover, following a path around the log-

arithmic branch cut at $z = 0$ connects the parity-broken solutions of the attractive and repulsive Hubbard models, completing a smooth manifold of solutions over the full parameter space.

Insights such as those presented above are not, however, restricted to a single occupied-virtual orbital rotation angle. Instead, they demonstrate a general framework for understanding the topology of real Hartree–Fock states. To emphasise this point, we apply the holomorphic Hartree–Fock framework to the two-electron, three-site periodic Hubbard chain, parameterised by the complex angles θ_1 and θ_2 using the exponential form of a complex-orthogonal matrix[30]

$$\left[\mathbf{C}_{\text{occ}}, \mathbf{C}_{\text{virt}}\right] = \exp \begin{pmatrix} 0 & \theta_1 & \theta_2 \\ -\theta_1 & 0 & 0 \\ -\theta_2 & 0 & 0 \end{pmatrix}. \tag{11}$$

To cover the full range of U/t values, we employ the parameterisation $(t, U) = (1 - |\epsilon|, \epsilon)$ where $\epsilon \in [-1, 1]$, and identify a total of 13 h-RHF solutions for all U/t values, as shown in Figure 3(a). An additional 47 h-UHF solutions can also be located, however these are omitted for clarity. Although obtaining analytic expressions for the h-RHF solutions is more challenging in this multiple variable system, the connectivity of Hartree–Fock states can still be explored by tracing the critical values of θ_1 and θ_2 for complex U/t values. Considering the repulsive regime, we observe the coalescence of a pair of solutions (each 3-fold spatially degenerate) at $(U/t)_{\text{CFP}} \approx 13.3$. Following a path around this Coulson–Fischer point in the complex U/t plane interconverts the two coalescing states after the first full rotation and returns them to their original state after the second, as shown in Figure 3(b). In doing so, we reveal a fundamental connection between two states that are completely unrelated by symmetry, and would otherwise only be associated through their coalescence.

Finally, we address the singularities in the holomorphic energies of the parity-broken states for both the two- and three-site systems as $U/t \to 0$. Inspection of the orbital coefficients reveals these singularities to be a manifestation of the self-orthogonality phenomenon,[16] where the wavefunction $|\psi\rangle$ satisfies $\langle\psi^*|\psi\rangle = 0$ (or for a holomorphic Hartree–Fock orbital $\sum_{\mu}^{n} C_{i\cdot}^{\mu} C_{\cdot i}^{\mu\cdot} = 0$). Within the projective space framework laid out in Ref. [24], self-orthogonal solutions correspond to "points at infinity". For linear non-Hermitian Hamiltonian, self-orthogonal eigenvectors occur when two solutions become equivalent at a branch point[16]. In contrast, the self-consistency of the Hartree–Fock equations leads to states that are in general non-orthogonal, and hence solutions may coincide without becoming self-orthogonal. However, removing all electron correlation in the limit $U/t \to 0$ leaves only the linear one-electron component in the Hamiltonian, and thus the states that coalesce at the logarithmic branch point in Figure 2 must become self-orthogonal. Mathematically, the absence of self-consistency requires solutions to share the symmetries of the one-electron Hamiltonian, requiring symmetry-broken states to be removed from the solution set by becoming self-orthogonal.

To summarise, we have demonstrated that holomorphic Hartree–Fock theory provides the analytic continuation of the real Hartree–Fock equations required for exploring the topology of multiple Hartree–Fock states. Exploiting this non-Hermitian framework in the periodic Hubbard chain exposes connections between real symmetry-broken states through the complex plane, along with self-orthogonal solutions in the correlation-free limit. These connections reveal an underlying continuous manifold of Hartree–Fock states and suggest alternative routes for identifying novel solutions through the complex direction. Moreover, whilst non-Hermitian Hartree–Fock resonance methods analytically continue electronic or atomic positions, the holomorphic Hartree–Fock approach explicitly continues only the orbital coefficients. Ultimately, unifying both approaches will reveal holomorphic solutions on the real axis in non-Hermitian Hartree–Fock and open new avenues for exploring the topology of multiple Hartree–Fock states in general.

H.G.A.B. thanks the Cambridge and Commonwealth Trust for a Vice-Chancellor's Award Scholarship and A.J.W.T. thanks the Royal Society for a University Research Fellowship (UF110161).

* hb407@cam.ac.uk

[1] Attila Szabo and Neil S. Ostlund, *Modern Quantum Chemistry* (Dover, 1989).
[2] A. J. W. Thom and M. Head-Gordon, Phys. Rev. Lett. **101**, 193001 (2008).
[3] K. Kowalski and K. Jankowski, Phys. Rev. Lett. **81**, 1195 (1998).
[4] A. T. B. Gilbert, N. A. Besley, and P. M. W. Gill, J. Phys. Chem. A **112**, 13164 (2008).
[5] D. Thouless, Nucl. Phys. **21**, 225 (1960).
[6] J. Čížek and J. Paldus, J. Chem. Phys. **47**, 3976 (1967).
[7] J. Paldus and J. Čížek, Chem. Phys. Lett. **3**, 1 (1969).
[8] R. Seeger and J. A. Pople, J. Chem. Phys. **66**, 3045 (1977).
[9] H. Fukutome, Int. J. Quantum Chem. **20**, 955 (1981).
[10] J. Stuber and J. Paldus, in *Fundam. World Quantum Chem. A Tribut. Vol. to Mem. Per-Olov Löwdin*, Vol. 1, edited by E. J. Brändas and E. S. Kryachko (Kluwer Academic, Dordrecht, 2003) pp. 67–139.
[11] P. Lykos and G. W. Pratt, Rev. Mod. Phys. **35**, 496 (1963).
[12] M. Mestechkin, Int. J. Quantum Chem. **15**, 601 (1979).
[13] M. Mestechkin, J. Mol. Struct. THEOCHEM **181**, 231 (1988).
[14] C. Coulson and I. Fischer, Philos. Mag. **40**, 386 (1949).
[15] C. W. McCurdy, T. N. Rescigno, E. R. Davidson, and J. G. Lauderdale, J. Chem. Phys. **73**, 3268 (1980).

[16] N. Moiseyev, *Non-Hermitian Quantum Mechanics* (Cambridge University Press, Cambridge, UK, 2011).
[17] C. M. Bender and S. Boettcher, Phys. Rev. Lett. **80**, 5243 (1998).
[18] C. M. Bender, D. C. Brody, and D. W. Hook, J. Phys. A: Math. Theor. **41**, 352003 (2008).
[19] C. M. Bender, Reports Prog. Phys. **70**, 947 (2007).
[20] C. M. Bender, J. Phys.: Conf. Ser. **631**, 012002 (2015).
[21] A. J. W. Thom and M. Head-Gordon, J. Chem. Phys. **131**, 124113 (2009).
[22] H. G. Hiscock and A. J. W. Thom, J. Chem. Theory Comput. **10**, 4795 (2014).
[23] H. G. A. Burton and A. J. W. Thom, J. Chem. Theory Comput. **12**, 167 (2016).
[24] H. G. A. Burton, M. Gross, and A. J. W. Thom, J. Chem. Theory Comput. **14**, 607 (2018).
[25] M. Head-Gordon, P. E. Maslen, and C. A. White, J. Chem. Phys. **108**, 616 (1998).
[26] W. Fischer and I. Lieb, *A Course in Complex Analysis* (Viewag+Teubner Verlag, 2012).
[27] B. D. Craven, J. Aust. Math. Soc. **10**, 341 (1969).
[28] F. Essler, H. Frahm, F. Gohmann, A. Klumper, and V. Korepin, *The One-Dimensional Hubbard Model* (Cambridge University Press, Cambridge, UK, 2005).
[29] We denote symmetry with respect to a centre of inversion between the two lattice sites. The correspondence to Bloch states is $\sigma_{\mathrm{g}} \equiv (k = 0)$ and $\sigma_{\mathrm{u}} \equiv (k = \pi/L)$ where L is the lattice site separation.
[30] F. R. Gantmacher, *The Theory of Matrices: Vol. II* (Chelsea, 1987).

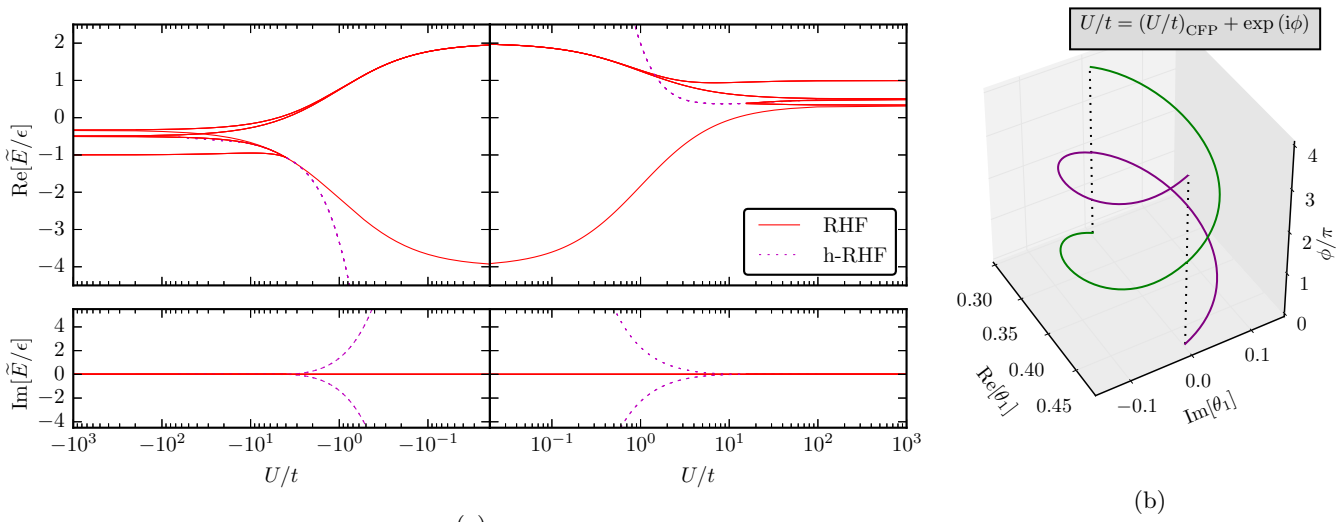

(a) (b)

FIG. 3: (a) Holomorphic energies of the 13 h-RHF solutions to the periodic three-site Hubbard chain with two-electrons using the parameterisation $(t, U) = (1 - |\epsilon|, \epsilon)$ where $\epsilon \in [-1, 1]$. The state degeneracies in order of ascending $\mathrm{Re}[\widetilde{E}/\epsilon]$ are 1, 3, 3, 3 and 3 in the $U/t \to \infty$ limit. (b) Critical θ_1 values for the pair of h-RHF states that coalesce at $(U/t)_{\mathrm{CFP}} \approx 13.3$ plotted along the path $U/t = (U/t)_{\mathrm{CFP}} + \exp(\mathrm{i}\phi)$ around the branch point. A single rotation interconverts the solutions, whilst a second rotation restores the original solutions.